ISSN 1075-7015, Geology of Ore Deposits, 2006, Vol. 48, No. 4, pp. 277–289. © Pleiades Publishing, Inc., 2006.
Original Russian Text © K.B. Bulnaev, 2006, published in Geologiya Rudnykh Mestorozhdenii, 2006, Vol. 48, No. 4, pp. 320–334.

Fluorine–Beryllium Deposits of the Vitim Highland, Western Transbaikal Region: Mineral Types, Localization Conditions, Magmatism, and Age

K. B. Bulnaev

Geological Institute, Siberian Division, Russian Academy of Sciences, ul. Sakh'yanovoi 6a, Ulan-Ude, 670047 Buryatia, Russia

Received March 27, 2006

Abstract—The fluorine–beryllium deposits of the Vitim Highland are represented by two mineral types: feldspar–fluorite–phenakite–bertrandite and thorite–fluorite–phenakite. Their localization is controlled by fault zones of various orders, folds, and stocks and dikes of the Early Mesozoic subalkali quartz syenite and syenite porphyry. The ore is represented by mineralized crush zones and metasomatic veins hosted in intercalated carbonate and aluminosilicate rocks. The deposits were formed under hydrothermal conditions at 360–90°C; their age is estimated at (243 ± 3)–(260 ± 2) Ma.

DOI: 10.1134/S1075701506040039

INTRODUCTION

The Aunik, Upper Amandak, and Amandak fluorine–beryllium deposits have been known in the northwestern Vitim Highland since the 1960s. The deposits of the fluorite–bertrandite–phenakite type (Ginzburg et al., 1975, 1977) are similar in formation and localization conditions and make up a common ore field. Nazarova (1965), having studied these deposits at the stage of their preliminary evaluation, showed that they are of hydrothermal origin and are closely related to minor stocklike quartz syenite and syenite porphyry intrusions and dikes. These statements were largely based on data from the Aunik deposit.

Our investigations included traditional methods: Rb–Sr dating of ore, analysis of REE patterns, and estimation of ore formation temperatures. The results obtained were discussed previously in consideration of the genesis of deposits (Bulnaev, 1996) and description of the Amandak deposit (Tsybzhitov, 1981). New data on the Rb–Sr age and the trace element geochemistry of intrusive rocks at the Aunik deposit were published by Lykhin et al. (2003).

GEOLOGY OF THE DISTRICT

The central part of the district is occupied by an Early Paleozoic geosynclinal trough filled by volcanic and terrigenous rocks with limestone interlayers (Fig. 1). This sequence overlies with stratigraphic and angular unconformity a Neoproterozoic metasedimentary complex that crops out at trough walls and in a narrow tectonic inlier within the trough (Osokin and Voyush, 1965).

The rocks of both complexes are deformed into large linear folds complicated by faults. The Neoproterozoic rocks are deformed most severely with formation of variously oriented folds. The folds in the Paleozoic trough extend in the northeastern direction.

Numerous faults of various scale, age, and depth of penetration are very important structural features. The NE-trending fault zones that bound on both sides the Paleozoic trough and the tectonic inlier within it are the most extended, widest, and longest lived. Early Mesozoic minor stocks and dikes of ore-bearing subalkali quartz syenite and related albitites are controlled by these faults and associated local fractures. An extended dikelike body of granite porphyry and quartz porphyry of the same age was mapped within the tectonic inlier located in the central part of the trough.

A Late Paleozoic (?) intrusive massif rounded in plan view and composed of granite and granodiorite was mapped at the drainage divide between the Bol'shaya Kira and Amandak rivers 2 km northwest of the Amandak deposit (Osokin and Voyush, 1965). According to recent data, this intrusion is composed largely of alkali pyroxene syenite and nepheline syenite and its age is regarded as Triassic. It cannot be ruled out that this intrusion is related to the same Early Mesozoic intrusive complex as the minor stocks and dikes.

LOCALIZATION CONDITIONS OF DEPOSITS

The Aunik and Amandak deposits are related to the marginal fault zones of the Paleozoic trough and to the contacts of alkali syenite stocks (Fig. 1). The poorly

Address for correspondence: K.B. Bulnaev. E-mail: gin@bsc.buryatia.ru

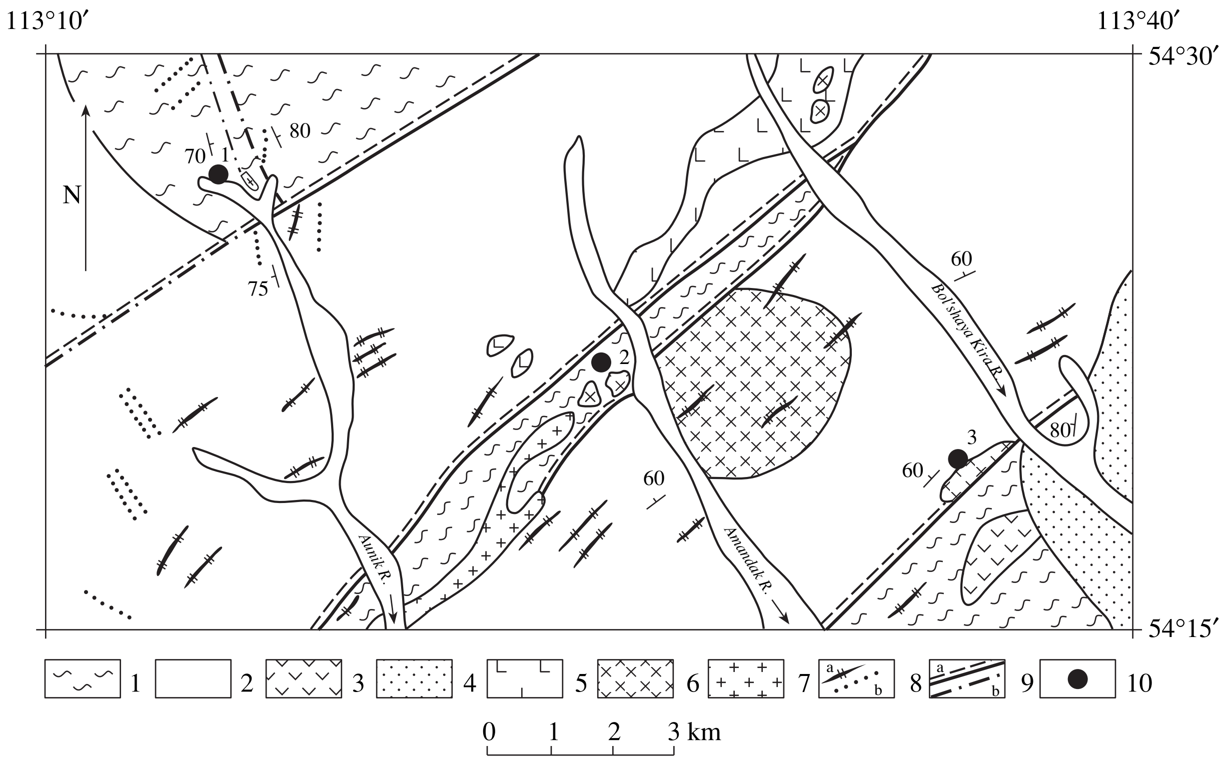

Fig. 1. Geological scheme of the ore district with fluorine–beryllium deposits of the Vitim Highland, modified after Osokin and Voyush (1965). (1) Alternation of crystalline limestone and carbonaceous–calcareous and phyllite-like slates and sandstone; (2) limestone, slate, sandstone, conglomerate, and basic and intermediate metavolcanics; (3) rhyolite, rhyolite porphyry, quartz porphyry, and rhyolitic tuff; (4) Quaternary sediments; (5) gabbro, gabbrodiorite, and diorite; (6) subalkali quartz syenite, syenite porphyry, and albitite; (7) granite porphyry; (8) dikes: (a) granite porphyry and (b) syenite porphyry; (9) faults: (a) mapped, (b) inferred; (10) fluorine–beryllium deposits (numerals in scheme): (1) Aunik, (2) Upper Amandak, (3) Amandak.

studied Upper Amandak ore occurrence occupies the same geological position within the aforementioned tectonic inlier of Precambrian rocks. In detail, the structural conditions and age of host rocks are different at particular deposits.

The Aunik deposit is located in the northwestern part of the ore district beyond the geosynclinal trough and hosted in complexly deformed Precambrian metasedimentary rocks (Fig. 2). The deposit is confined to the core of a small anticline composed of limestones alternating with carboniferous–calcareous and quartz–chlorite slates and polymictic sandstones. The fold extends in the northwestern direction and abuts against the trough structure. Ore-bearing fault-line intrusive bodies and branching lenticular lodes of F–Be ore are oriented in the same direction.

In contrast to the Aunik deposit, the Amandak deposit is situated at the opposite wall of the trough on the inner side of a boundary fault (Fig. 3). The deposit is related to the southeastern limb of an anticline composed of dolomitized limestone that is overlain by intercalating limestones and calcareous sandstones, which give way further upsection to polymictic sandstone with interlayers of calcareous shale. The fold strikes in the northeastern direction conformably with the trough axis and the boundary fault. The anticline is cut through by two stocks of quartz syenite and albitite different in size and syenitic dikes elongated in the same direction.

The largest of numerous faults are represented by conformable crush zones. Vein-shaped and lenticular orebodies are hosted in marmorized limestone of one such zone located between quartz syenite and albitite stocks. NW-trending and near-meridional faults are postmineral. They cut and displace the crush zones and related orebodies.

Thus, the deposits are controlled by deep fault zones that bound the Paleozoic trough and by a system of related splays. In both cases, the deposits are confined to small anticlines. Thereby, the fluorine–beryllium ore mineralization concentrates near contacts of minor quartz syenite and syenite porphyry intrusions, being hosted in intercalated carbonate and aluminosilicate rocks.

INTRUSIVE ROCKS

As was mentioned above, the igneous rocks at the F–Be deposits of the Vitim Highland are represented by

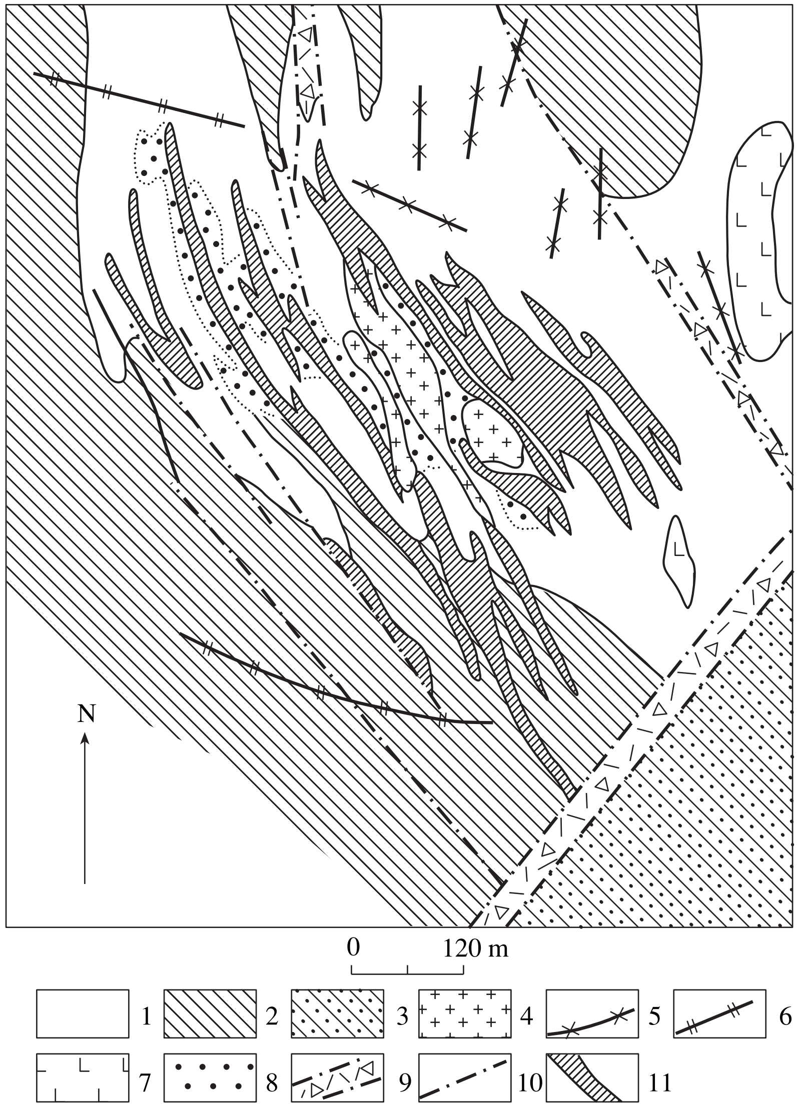

Fig. 2. Geological scheme of the Aunik fluorine–beryllium deposit, after E.I. Galkin and A.F. Zuev. (1) Limestone with slate interlayers, (2) carbonaceous–calcareous slate with limestone interlayers, (3) polymictic sandstone, (4) quartz syenite and syenite porphyry, (5) syenite porphyry dikes, (6) felsitic syenite porphyry dikes, (7) kersantite, (8) skarn and skarnified limestone, (9) crush and breccia zones, (10) fault, (11) orebody.

stocks and dikes of quartz syenite. Leucocratic quartz syenite, syenite porphyry, and kersantite compose ore-bearing intrusions at the Aunik deposit. According to our data, all these rocks were formed almost simultaneously and are regarded as facies varieties, in contrast to the view of Nazarova (1965), who considered these rocks to be discrete intrusive phases.

As can be clearly seen in exploration trenches, quartz syenite in cores of the largest stocks grades into syenite porphyry of similar composition in the contact zones. Smaller dikelike bodies consist of the same syenite porphyry. A similar facies change of intrusive rocks was established at the Yermakovka F–Be deposit, which has much in common with the Aunik deposit. The ore-bearing intrusion of subalkali leucogranite at the Yermakovka deposit grades into quartz syenite and syenite porphyry at contacts with carbonate rocks (Novikova et al., 1994).

Two small stocks and several dikes of kersantite are known at the Aunik deposit. They also cut through limestone at a distance from quartz syenite and syenite porphyry intrusions (Fig. 2). Kersantite contains numerous limestone xenoliths, and contamination of granitic melt with carbonate material was regarded as a mechanism of syenite formation (Nazarova, 1965).

The dikes that are located at the northeastern limb of the anticline and cut limestone are composed of syenite porphyry, whereas the dikes at the opposite limb, which are fewer in number and cut polymictic sandstone, consist of felsitic syenite porphyry. Both dike clusters are

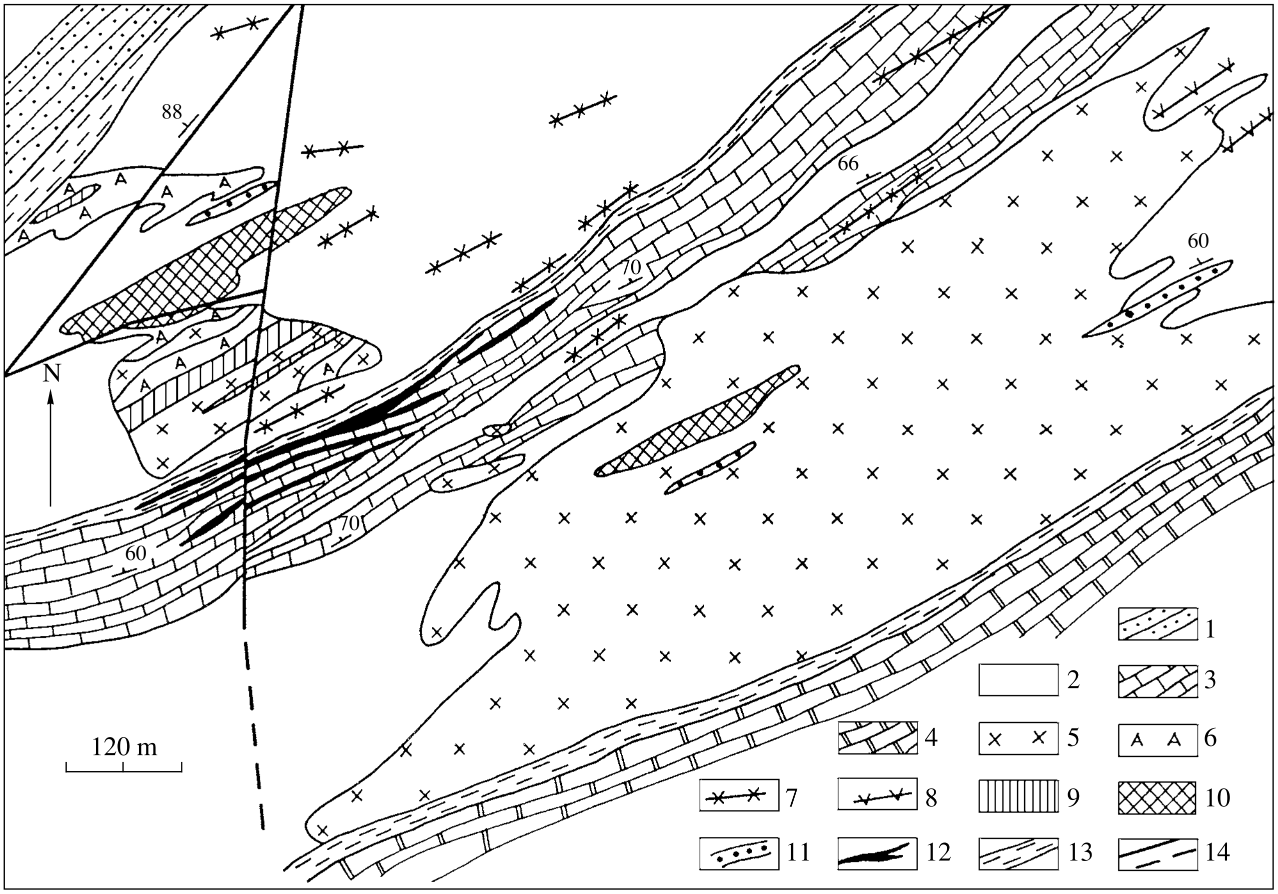

Fig. 3. Geological scheme of the Amandak fluorine–beryllium deposit. (1) Polymictic sandstone; (2) quartz–carbonate slate and sandstone partly transformed into hornfels with lenses of bituminous limestone; (3) marmorized and silicified limestones; (4) dolomite and dolomitized limestone; (5) subalkali quartz syenite locally albitized; (6) albitite; (7) quartz porphyry, microsyenite, and albitite dikes; (8) microdiorite dikes; (9) zone of tantalum mineralization; (10) zone of lithium mineralization; (11) zones of molybdenum mineralization; (12) fluorine–beryllium orebody; (13) brecciated zone; (14) faults.

situated at a distance from ore-bearing stocks and orebodies localized nearby. The crosscutting relations of auxiliary thin zones of F–Be mineralization to the dikes testify to the premineral character of the latter. At the same time, the dikes of felsitic syenite porphyry cut stocks of ore-bearing quartz syenite.

According to the data reported by Nazarova (1965), quartz syenite is a heterogeneous fine-grained rock often affected by metasomatic alteration. Microcline—the main rock-forming mineral—is partly replaced with albite; the quartz content is not higher than 8–10 vol %. Zircon, ferrithorite, monazite, and ilmenorutile are accessory minerals.

Quartz syenite is characterized by elevated Na_2O and K_2O contents with a slight prevalence of Na_2O over K_2O and is enriched in SrO (Table 1). In the TAS classification diagram, the chemical composition of rock falls into the field of subalkali granite (Fig. 4), and it corresponds to alkali feldspar granite and microcline–albite granite (albitized variety) in other classifications (Bogatikov et al., 1981; *Petrographic* …, 1995).

This rock was originally called subalkali quartz syenite on the basis of petrographic examination (Nazarova, 1965). In the absence of new data on the modal composition of the rock, it seems reasonable to retain this name. Quartz syenite contains 0.29–1.10 wt % F and 15 ppm Be (Table 2).

Syenite porphyry in contact zones and in separate minor intrusions consists of relatively large microcline and less frequent pyroxene phenocrysts incorporated into a holocrystalline groundmass composed of albitized microcline in association with quartz (up to 10 vol %), biotite (5–7%), fluorite, and calcite with accessory rutile, zircon, and apatite.

Syenite porphyry is distinguished from quartz syenite by a higher alkalinity and a lesser amount of silica (Table 1). In the classification diagram (Bogatikov et al., 1981), the chemical compositions of syenite por-

Table 1. Chemical composition of intrusive rocks at the fluorine–beryllium deposits of the Vitim Highland, wt %

Component	1	2	3	4	5	6	7	8	9	10
SiO_2	70.51	70.80	70.70	59.00	58.90	58.40	67.86	68.14	67.20	67.40
TiO_2	0.21	0.07	0.06	0.58	0.55	0.48	0.18	0.17	0.15	0.17
Al_2O_3	13.52	14.00	12.20	16.46	16.60	16.20	16.10	16.13	15.40	16.81
Fe_2O_3	1.07	0.19	0.84	1.60	1.96	1.52	0.99	0.91	1.56	1.22
FeO	2.16	2.01	2.79	2.94	3.13	3.21	0.83	0.92	0.62	0.73
MnO	0.16	0.04	0.14	0.23	0.20	0.17	0.05	0.03	0.04	0.02
MgO	0.09	0.06	0.46	0.36	0.37	0.33	0.31	0.40	0.56	0.44
CaO	0.83	0.27	0.63	1.85	1.54	1.92	2.68	2.38	2.44	2.47
Na_2O	4.38	4.47	4.20	5.30	5.28	5.47	5.53	6.00	5.77	5.78
K_2O	4.30	4.22	4.00	5.44	5.39	5.83	1.91	1.50	1.60	1.47
P_2O_5	0.01	0.01	0.04	0.09	0.11	0.13	0.03	0.06	0.08	0.08
LOI	2.28	2.62	2.52	3.10	3.04	2.86	2.84	2.61	2.86	2.18
CO_2	–	0.39	0.47	0.99	0.97	0.97	–	–	0.56	0.39
SO_3	0.30	0.25	0.20	1.19	1.35	1.54	0.48	0.28	0.91	0.39
$–O=F_2$	0.12	0.16	0.46	0.49	0.42	0.53	0.03	–	0.06	0.10
Total	99.99	99.61	99.89	99.80	99.97	99.75	99.83	99.53	99.83	99.69
Na_2O/K_2O	1.02	1.06	1.05	0.97	0.98	0.94	2.90	4.00	3.61	3.93
Component	11	12	13	14	15	16	17	18	19	20
SiO_2	47.00	67.20	67.60	68.28	69.40	69.50	68.61	68.22	65.21	65.84
TiO_2	1.36	0.11	0.13	0.15	0.10	0.13	n.d.	0.05	0.05	0.12
Al_2O_3	15.20	15.90	15.40	15.98	16.00	15.95	18.00	18.64	18.92	18.98
Fe_2O_3	5.25	2.48	2.54	1.77	2.07	1.90	0.97	1.19	1.11	1.46
FeO	0.81	0.39	0.77	0.51	0.40	0.52	0.29	0.22	0.43	0.86
MnO	0.20	0.06	0.08	0.08	0.07	0.09	tr	tr	0.06	0.01
MgO	2.07	0.09	0.10	tr	0.01	n.d.	0.09	tr	0.20	n.d.
CaO	4.69	0.57	0.41	0.75	0.62	n.d.	0.37	0.17	1.33	1.04
Na_2O	4.06	6.13	5.91	5.62	6.25	0.56	9.49	9.62	10.23	10.10
K_2O	5.81	5.05	4.66	4.49	4.05	5.55	0.28	0.31	0.38	0.45
P_2O_5	0.45	0.02	0.04	0.01	n.d.	4.35	0.05	0.02	0.03	0.05
LOI	2.29	1.24	1.49	1.59	1.14	0.01	1.05	0.88	1.14	–
CO_2	3.47	–	–	–	–	1.39	–	–	–	–
SO_3	6.52	0.20	0.20	0.25	0.10	0.05	0.25	0.20	0.45	0.85
$–O=F_2$	0.18	0.17	0.22	0.15	0.15	–	0.01	0.01	0.33	n.d.
Total	99.42	99.61	99.55	99.63	100.36	99.80	99.47	99.53	99.87	99.76
Na_2O/K_2O	0.70	1.21	1.27	1.25	1.54	1.28	33.89	31.03	26.92	22.44

Note: The Aunik deposit: (1–3) subalkali quartz syenite, (4–6) syenite porphyry, (7–10) felsitic syenite porphyry (dikes), (11) kersantite; the Amandak deposit: (12–16) albitized quartz syenite, (17–20) albitite; n.d., not detected; a dash denotes not analyzed. Analyses were performed at the chemical laboratory of the Geological Institute, Siberian Division, Russian Academy of Sciences, Ulan-Ude; analysts, V.A. Ivanova and N.L. Guseva.

phyry fall in the field of syenite far from compositions of quartz syenite (Fig. 4). The F contents in both rocks are comparable, but syenite porphyry is enriched in Be (23 ppm, on average; Table 2).

The dikes of felsitic syenite porphyry have an aphanitic groundmass and small microcline phenocrysts. They contain more SiO_2 and Na_2O but the K_2O content is lowered (Table 1). In the TAS diagram, their compositions are localized near the field of subalkali granite (Fig. 4).

Kersantite from stocks and dikes is also a porphyritic rock (Table 1). Phenocrysts are represented by pla-

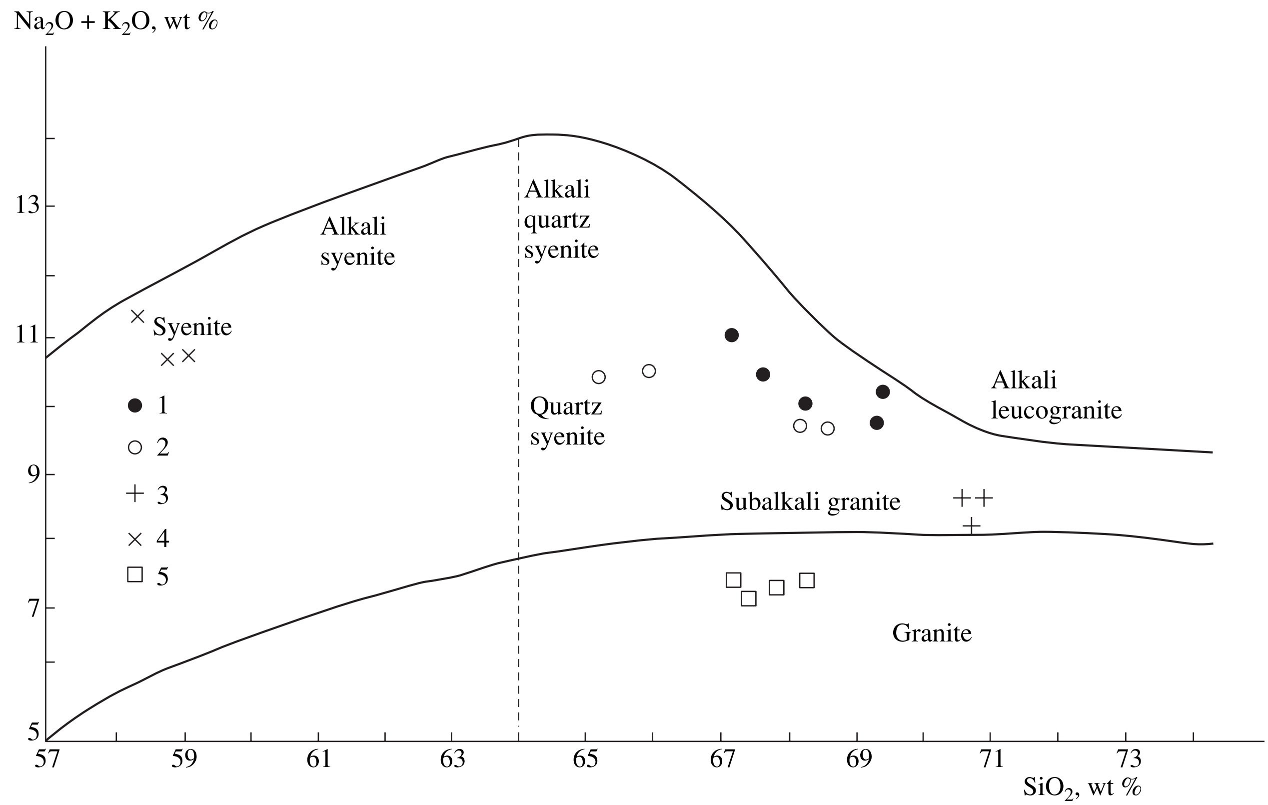

Fig. 4. Chemical compositions of intrusive rocks from fluorine–beryllium deposits plotted on the TAS diagram. Amandak deposit: (1) subalkali quartz syenite, (2) albitite. Aunik deposit: (3) subalkali quartz syenite, (4) syenite porphyry, (5) felsitic syenite porphyry.

gioclase, biotite, and less frequent pyroxene and quartz, and the groundmass consists of plagioclase and biotite occasionally replaced with calcite and epidote; abundant fine disseminations of pyrite are typical.

Table 2. Average F and Be contents in intrusive rocks at the fluorine–beryllium deposits of the Vitim Highland, wt %

Deposit and rock	Number of samples*	F	Be
Amandak deposit			
Albitized quartz syenite	17/12	0.18	0.0010
Albitite	40/11	0.05	0.0017
Eruptive breccia	2/4	1.51	0.0024
Aunik deposit			
Quartz syenite	18/7	0.333	0.0015
Syenite porphyry	14/6	0.325	0.0023
Felsitic syenite porphyry	12/8	0.185	0.0020
Pyritized kersantite	5/3	0.236	0.0020

* The number of F determinations is given in the numerator and the number of Be determinations, in the denominator.

By $Na_2O + K_2O$ sum, the rock occupies a transitional position between albitized quartz syenite and syenite porphyry.

At the Amandak deposit, the intrusive rocks comprise two quartz syenite stocks different in size; a dike-shaped albitite body; and a series of microdiorite, microsyenite, and albitite dikes (Fig. 3). The larger stock of quartz syenite, about 0.5 km^2 in size, cuts through polymictic sandstone with interlayers of carbonate rocks. Garnet–diopside and garnet–diopside–vesuvianite skarn bodies are developed at intrusive contacts with limestone. Two small outcrops of quartz syenite at the sandstone/limestone interface are offsets of the uneven surface of the main stock, which dips to the northwest at angles of 55°–70°.

The smaller stock of quartz syenite is situated to the northwest of the larger one and separated from the latter by a narrow tract of marmorized limestone. The same sandstone serves as country rock. The stock is located in a narrow tectonic block bounded by near-latitudinal faults on both sides.

As at the Aunik deposit, microcline and albite are the major rock-forming minerals of quartz syenite. Quartz occurs as sporadic grains, and dark-colored minerals are lacking.

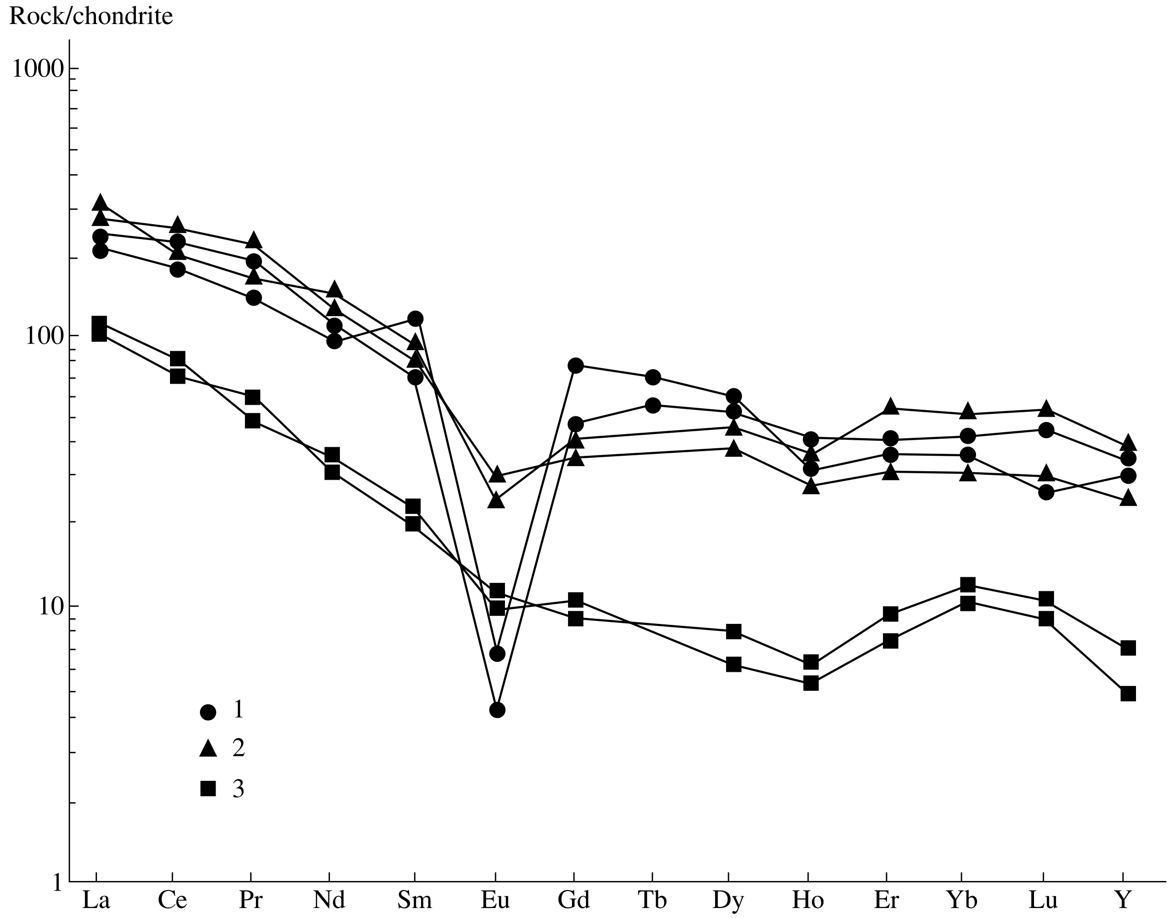

Fig. 5. Chondrite-normalized REE patterns of intrusive rocks from the Aunik deposit. (1) Subalkali quartz syenite, (2) syenite porphyry, (3) felsitic syenite porphyry (dikes).

Widespread sodic metasomatism is typical, and a small dikelike albitite body at the northwestern flank of the deposit is related to this process. Zones of metasomatic rocks similar in composition were established in quartz syenite of the smaller stock.

The chemical composition of albitized quartz syenite at the Amandak deposit is similar to its analogue at the Aunik deposit. The metasomatic rocks at the Amandak deposit are only distinguished by a lower SiO_2 content along with an elevated $Na_2O + K_2O$ sum and by a greater prevalence of Na_2O over K_2O (Table 1). The F content varies from 0.12 to 0.26 wt % (0.18 wt %, on average; Table 2). The average Be content amounts to 10 ppm.

In the TAS diagram, the compositions of quartz syenite are clustered between standard quartz syenite and subalkali granite, closer to the former, while the albitite compositions mostly fall into the field of quartz syenite. Thus, the intrusive rocks at the Amandak deposit should be classified as subalkali quartz syenite.

The chondrite-normalized REE patterns of quartz syenites from both deposits are broadly similar (Figs. 5, 6a). The chondrite-normalized REE contents gradually decrease from La to Lu in combination with a deep Eu minimum and a poorly expressed Ho minimum. The REE pattern of syenite porphyry from the Aunik deposit is similar to that of quartz syenite but the Eu minimum is less distinct. The late felsitic syenite porphyry is devoid of a Eu minimum and distinguished by a lower general level of REE contents, gradually decreasing from La to Ho; the Er, Yb, and Lu contents are slightly elevated.

The REE distribution in albitites of the Amandak deposit is nonuniform (Fig. 6b). The LREE contents are approximately the same as in quartz syenite; the Eu minimum is clearly delineated. Concentrations of MREE and LREE are less consistent and often elevated due to the appearance of accessory monazite, allanite, and bastnaesite.

In general, the similar level of REE concentration and chondrite-normalized REE patterns of quartz syenite and syenite porphyry confirms the comagmatic nature of these rocks.

The alkali and subalkali granites of the Vitim Highland were previously considered as constituents of the

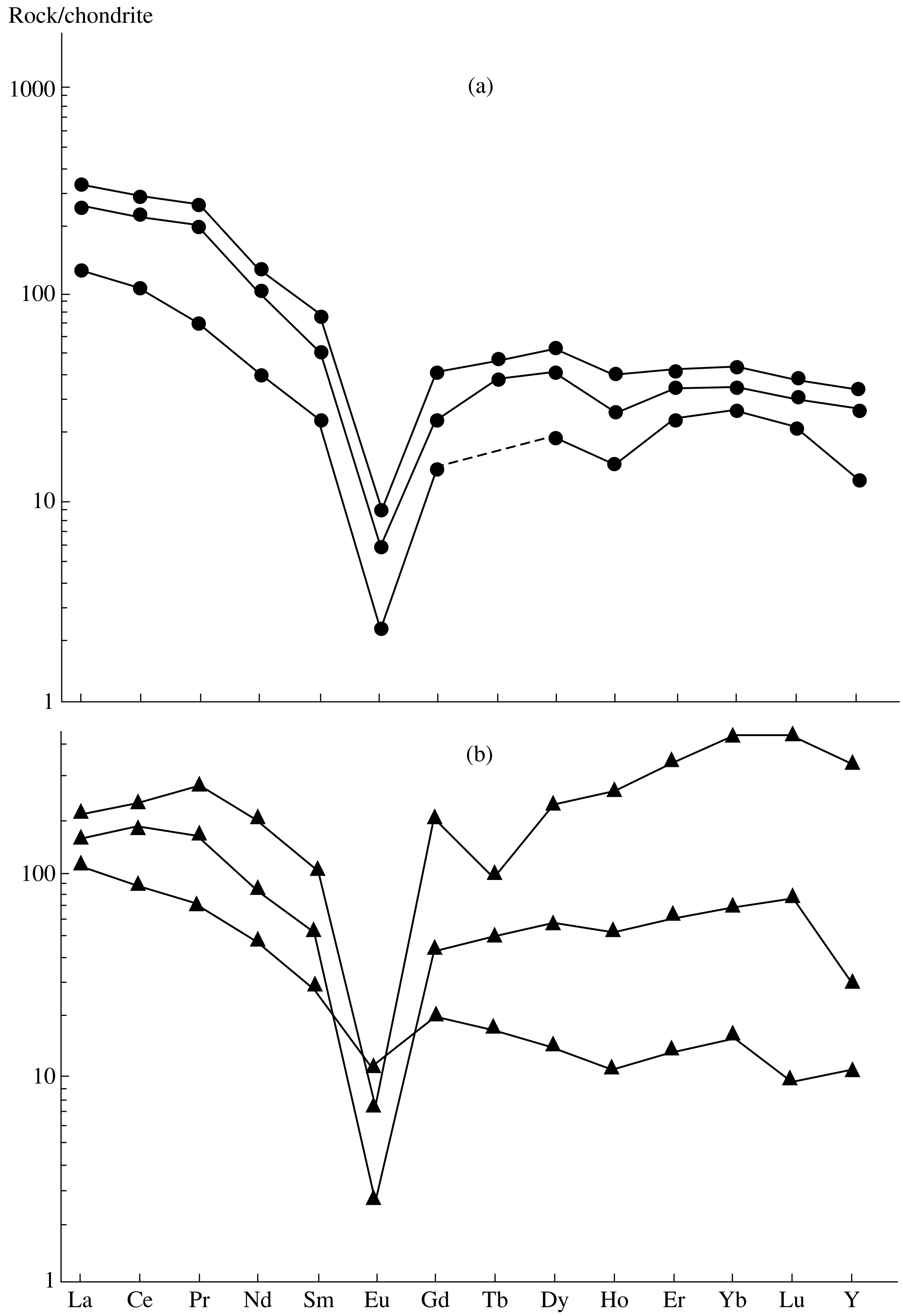

Fig. 6. Chondrite-normalized REE patterns of rocks from the Amandak deposit. (a) Subalkali quartz syenite, (b) albitite.

transregional Permian–Triassic Mongolian–Transbaikal belt of alkaline granitoids (Zanvilevich et al., 1975). Subsequently, it was established that granitoid rocks of the western Transbaikal region are mostly Early Mesozoic in age (Yarmolyuk et al., 2001). The Rb–Sr age of intrusive rocks at the Aunik deposit was recently estimated at 241 ± 1.6 Ma (Lykhin et al., 2003).

OREBODY FORMATION

The fluorine–beryllium deposits of the Vitim Highland, despite their similarity in geology, relationships with igneous rocks, mineral composition, and formation conditions, nevertheless reveal some local differences. About ten orebodies variable in thickness and extent were contoured at the Aunik deposit (Fig. 2). The complexly shaped lenticular lodes, often branching along the strike, concentrate near contacts of ore-bearing quartz syenite and syenite porphyry stocks. The orebodies are hosted in massive limestone with interlayers of carboniferous–calcareous and phyllite-like slates occasionally transformed into hornfels and actinolite–vesuvianite skarn. The southeastern ends of some orebodies enter into polymictic sandstone.

The orebodies are mineralized crush zones up to 500 m in extent. Metasomatic veins of rhythmically banded ore are hosted in homogeneous marmorized limestone and composed of dark violet fluorite (72%) and narrow light bands that additionally contain microcline (3.4%), quartz (4.1%), and phenakite or albite and bertrandite.

The ore breccia predominant in mineralized zones consists of fragments of limestone replaced with fluorite, calcareous slate, skarn, and quartz syenite cemented with a calcite–fluorite–albite–bertrandite aggregate. Late carbonate veinlets and lenticular segregations contain abundant pyrite disseminations and sporadic grains of galena, sphalerite, and molybdenite. The thickness of mineralized zones is variable and decreases down the dip on approaching the intrusive stock.

Two stages of ore deposition different in alkali metal activity were recognized previously (Nazarova, 1965). According to our data, this process proceeded in a disturbed tectonic setting during three stages: (1) quartz–microcline–fluorite–phenakite at 360–310°C, (2) albite–fluorite–bertrandite at 140–90°C, and (3) carbonate–sulfide at 130–100°C.

Until recently, the Amandak deposit was considered a close analogue of the Aunik deposit and both were classified as belonging to the feldspar–fluorite–phenakite–bertrandite type (Nazarova, 1965). However, the results of subsequent exploration and our studies have shown that this deposit substantially differs from the Aunik deposit in mineral composition of ore and pertains to the thorite–fluorite–phenakite type.

Ten orebodies up to 260 m in extent and varying in thickness from 0.1–0.2 to 4.0–7.0 m were contoured as a result of geological exploration. They are metasomatic veins of complicate morphology hosted in marmorized limestone that intercalates with quartz–carbonate sandstones in the area between stocks of quartz syenite (Fig. 3). In sandstones and other aluminosilicate rocks, including skarn bodies, the ore mineralization bears a stringer–disseminated character. Fracture and crush zones are important as factors of ore localization.

The mineral composition of ore at the Amandak deposit is rather complex and variable. In addition to the prevalent fluorite (77.5%) and phenakite (up to 3%), thorite, bertrandite, K-feldspar, quartz, and carbonate are noted in small amounts, as well as still less abundant pyrite, galena, sphalerite, molybdenite, and biotite. Zircon, monazite, allanite, bastnaesite, scheelite, rutile, apatite, and zinnwaldite were identified as accessory minerals.

It was established that the thorite–fluorite–phenakite mineralization was formed during two stages divided by tectonic motions (Tsybzhitov, 1981). The main fluorine–beryllium ore was formed at the initial stage, whereas monomineral fluorite or quartz–fluorite veins are products of the second stage.

As follows from results of fluid inclusion study, the minerals of the first stage crystallized at 290–190°C. Fluid inclusions contained in phenakite from this mineral assemblage are homogenized at 220–200°C. The coarse-grained fluorite of the second stage was deposited at 190–130°C.

The chemical composition of brecciated ore at the Aunik deposit is extremely unstable and varies depending on the contribution of lithic fragments. The F grade varies from 5–6 to 14.5–18.0 wt %, whereas the grade of massive metasomatic ore increases to 32 wt % (Table 3). The analysis of two technological samples from the ore of both types yielded 0.20 wt % BeO.

The composition of massive F–Be ore from metasomatic veins at the Amandak deposit is close to that at the Aunik deposit, including the fluorite content. The BeO content varies from 0.16 to 4.72 wt %.

The chondrite-normalized REE and Y patterns of massive ore from both deposits are similar (Figs. 7a, 7b). They are characterized by a deep Eu minimum and elevated MREE, HREE, and Y contents in comparison with ore-bearing intrusive rocks. The ore of the Amandak deposit reveals an increase in Nd, Sm, Yb, and Lu contents.

As was established by drilling results, the feldspar–fluorite–phenakite–bertrandite ore that occurs at the upper levels of the Aunik deposit grades with depth into albite–fluorite–phenakite ore. Judging by the distribution of mineral types of ore and the morphology and dimensions of ore-bearing intrusions, the Amandak deposit with its thorite–fluorite–phenakite ore was eroded more deeply than the Aunik deposit.

The fluorine–beryllium ore mineralization at the deposits of the Vitim Highland is often accompanied by ore mineralization of other types. Attendant rare-metal mineralization is developed especially intensely at the Amandak deposit, where it is related to albitized crush zones in quartz syenite and polymictic sandstone (Fig. 3).

Three lenses of pegmatoid albitites with zircon, xenotime, columbite, cassiterite, pyrite, and fluorite disseminations were established in the smaller stock of quartz syenite located in the northwestern part of the

Table 3. Chemical composition of massive fluorine–beryllium ores from the Amandak and Aunik deposits, wt %

Component	1	2	3	4	5	6
SiO_2	16.30	15.20	15.10	18.10	18.40	17.80
TiO_2	0.15	0.05	0.18	0.12	0.08	0.77
Al_2O_3	3.24	3.07	4.22	5.90	5.91	5.80
Fe_2O_3	0.52	0.40	0.65	1.70	1.16	0.53
FeO	n.d.	n.d.	n.d.	0.35	1.35	0.85
MnO	0.12	0.12	0.13	0.02	0.09	0.05
MgO	0.11	0.10	0.10	0.43	0.56	0.47
CaO	54.50	55.00	54.10	48.20	49.22	48.70
Na_2O	0.24	0.20	0.21	0.28	4.17	0.01
K_2O	2.15	1.93	2.70	1.34	0.25	0.09
P_2O_5	0.41	0.26	0.64	1.10	0.92	1.14
CO_2	n.a.	n.a.	0.78	0.20	2.14	1.75
SO_3	″	″	n.a.	1.60	3.80	0.73
F	32.00	33.50	32.00	31.00	14.50	32.00
$–O=F_2$	13.44	14.07	13.44	13.02	6.09	13.44
Total	96.30	95.76	97.37	97.32	96.46	97.25

Note: Deposits: (1–3) Amandak; (4–6) Aunik; n.d., not detected; n.a., not analyzed. Analyses were performed at the chemical laboratory of the Geological Institute, Siberian Division, Russian Academy of Sciences, Ulan-Ude; analyst, A.A. Tsyrenova.

deposit. The lenses vary from 10 to 12 m in thickness and contain (wt %) 0.015 Ta_2O_5, up to 1.0 Zr and Th, and 0.59–0.88 REE.

A zone of Li mineralization, up to 40 m thick, was revealed in the albitized polymictic sandstone and eruptive breccia close to the northern contact of the stock mentioned above. The mineralized rocks contain flakes of lepidolite and Li-bearing muscovite. Emission spectroscopy recorded 0.52–0.91 wt % Li; up to 1 wt % Zr and Th; and tenths and hundredths of percent of Nb, Sn, Pb, and Y. Similar ore mineralization was detected in the northwestern portion of the main quartz syenite stock.

Orebodies of the Amadak deposit are also enriched in Li and Th (up to 1 wt %) owing to the occurrence of zinnwaldite and more abundant thorite.

A zone of molybdenite mineralization with 0.02–0.80 wt % Mo was penetrated by boreholes at a depth of 145–190 m in the contact zone of albitized and silicified quartz syenite at the Aunik deposit. Molybdenite is contained in numerous quartz veinlets in association with galena, sphalerite, and arsenopyrite. Furthermore, the silicified apical zone of a small quartz syenite stock penetrated by boreholes also bears molybdenite. It is noteworthy that neither in the first nor in the second case are the molybdenite occurrences accompanied by F–Be mineralization. These two types of ore mineralization are separated in space: Mo is concentrated largely in contact zones of intrusions, while F and Be occur at some distance from intrusive contacts.

Rb–Sr AGE OF ORE MINERALIZATION

Until now, the age of F–Be deposits of the Vitim Highland has been accepted as Early Mesozoic, assuming their genetic or paragenetic links with granitoids that were suggested to be of the same age. In this regard, it was important to estimate the age of ore directly.

Whole-rock samples of feldspar–fluorite–phenakite–bertrandite ore in combination with feldspar and fluorite monofractions were used for this purpose at the Aunik deposit and thorite–fluorite–phenakite ore, biotite, and fluorite from the Amandak deposit.

The isotopic composition of Sr, as well as Rb and Sr contents, were determined on a MI-1201T single-collector mass spectrometer combined with a PRM-2 system of automatic registration based on PC Iskra-1256. The Sr isotopic composition and its content were determined with the method of double isotope dilution, and the Rb concentration, with the isotope dilution method. The uncertainties of analysis of the Sr isotopic composition and the $^{87}Rb/^{86}Sr$ ratio were not worse than 0.05 and 1.0%, respectively, at a 95% confidence level. At the moment of measurements, the $^{87}Sr/^{86}Sr$ ratio in the VNIIM (All-Russia Research Institute of Metrology) standard was 0.70797 ± 0.00008.

The Rb–Sr data obtained as a result of measurements (Table 4) are shown as graphs in Fig. 8. The age was calculated with the ISOPLOT program. For the Aunik deposit, two age estimates of 257 and 243 Ma and a common I_{Sr} = 0.7089 were obtained using two

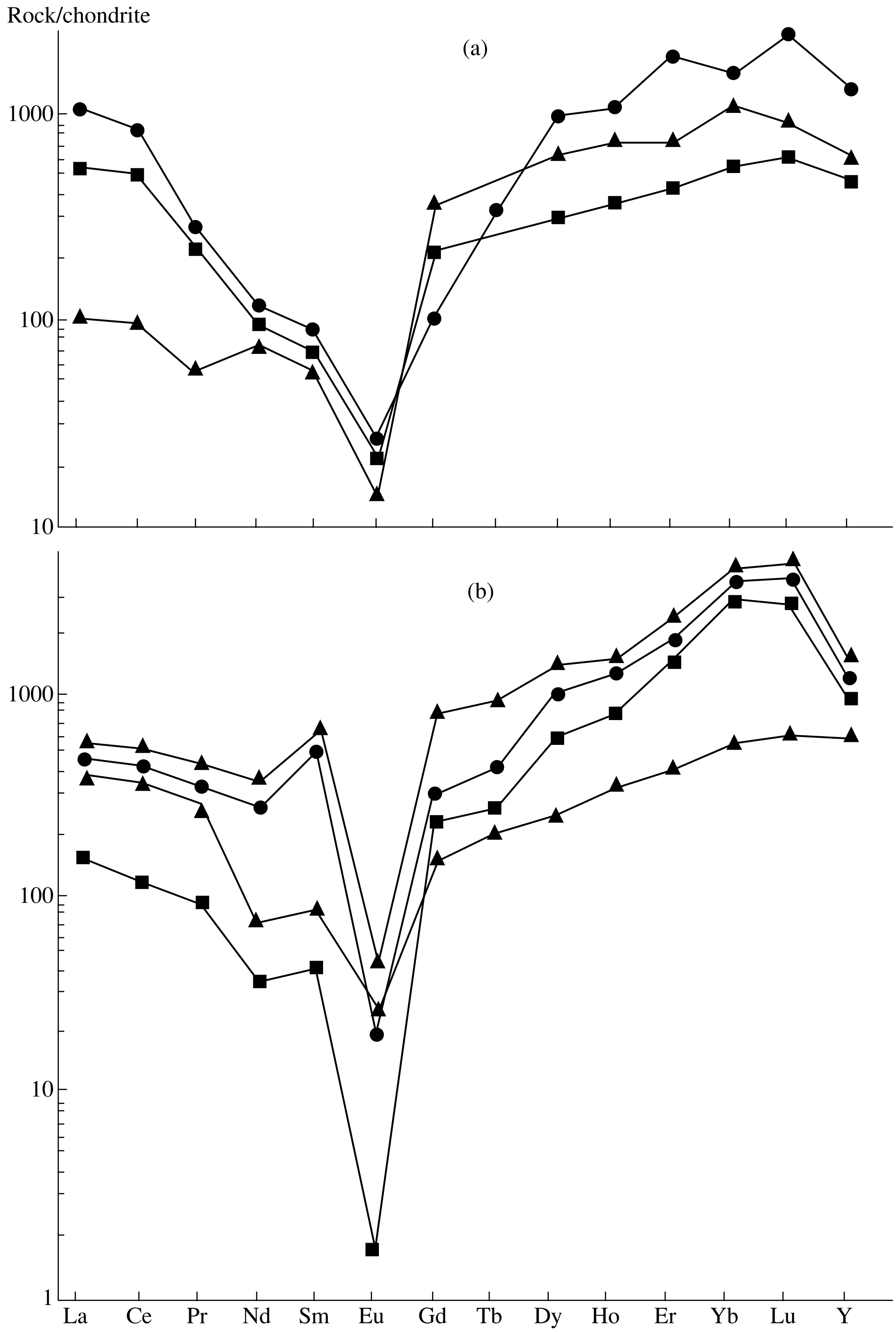

Fig. 7. Chondrite-normalized REE patterns of ores from the (a) Aunik and (b) Amandak fluorine–beryllium deposits.

K-feldspar samples combined with a whole-rock sample and two fluorite monofractions (Fig. 8a). The difference in age could be related either to nonsynchronous closure of the Rb–Sr system in feldspars or to the effect of superimposed processes. An isochron that corresponds to the age 260 ± 2 Ma and I_{Sr} = 0.7087 ± 0.0002 was obtained for the Amandak deposit.

Hence, it may be stated that the F–Be deposits under consideration were formed virtually simultaneously,

Table 4. Rb and Sr contents and Sr isotopic composition of ores and ore-forming minerals from the Aunik and Amandak deposits

Deposit	Sample	Material	Rb, ppm	Sr, ppm	$^{87}Rb/^{86}Sr$	$^{87}Sr/^{86}Sr$
Aunik	Au-21	Ore	603.8	2696.9	0.6505	0.71135
"	Au-27	K-feldspar	2453.5	59.49	124.6	1.16524
"	Au-40	"	2566.5	21	401.5	2.09844
"	Au-45	Fluorite	22.56	2885.9	0.02262	0.70897
"	Au-47	"	51.18	3759.4	0.03938	0.70896
Amandak	Am-99	Ore	166.9	4011.4	0.1204	0.70909
"	Am-30	Biotite	2592.2	45.65	174.6	1.34886
"	Am-31	"	2572.5	24.6	339.9	1.97227
"	Am-23	Fluorite	18.6	4837.3	0.01112	0.70872
"	Am-25	"	9.078	3594.1	0.0073	0.70874

although they are located 40 km apart from each other and are hosted in different metasedimentary rocks. The age of the deposits was probably controlled by the time of emplacement of subalkali granitoids.

The Rb–Sr age of deposits turned out to be somewhat older than that estimated by Lykhin et al. (2003) for quartz syenite and syenite porphyry at the Aunik deposit (241.6 ± 1.6 Ma). In my opinion, this insignificant discrepancy is caused by the determination of the Rb–Sr age largely by K-feldspar from quartz syenite affected by hydrothermal alteration. Lykhin et al. (2003) also estimated the Rb–Sr age of kersantite from

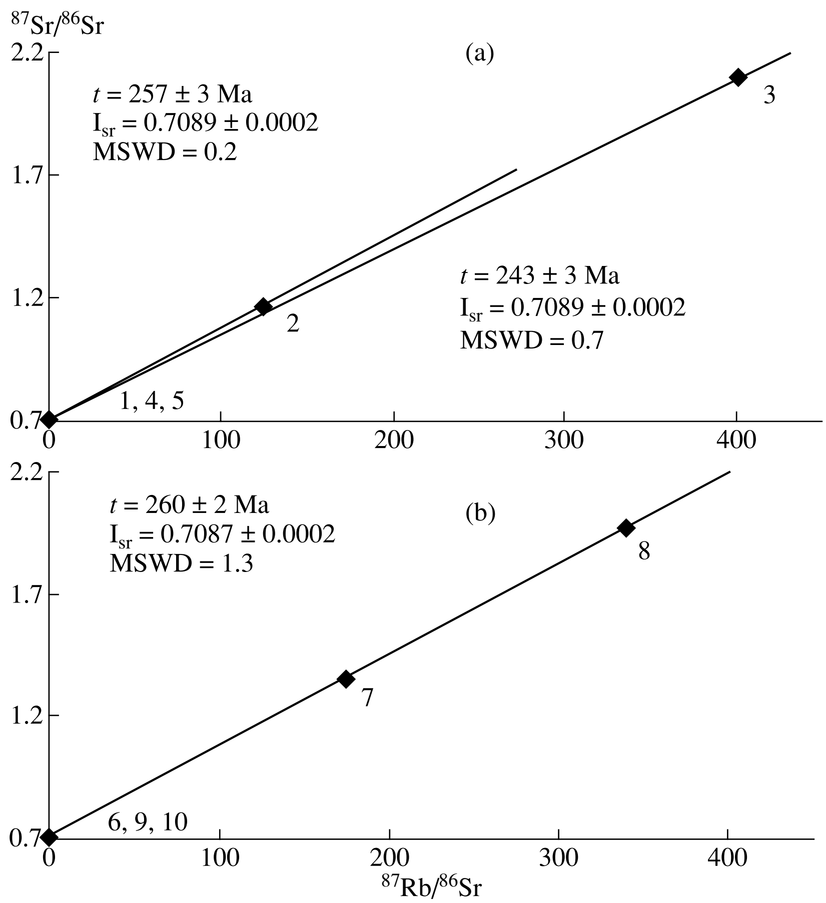

Fig. 8. Rb–Sr isochrons of the (a) Aunik and (b) Amandak fluorine–beryllium deposits. (1) Ore, (2, 3) K-feldspar, (4, 5) fluorite, (6) ore, (7, 8) biotite, (9, 10) fluorite.

the Aunik deposit at 276 ± 20.2 Ma. In this regard, it is worth noting that, at several localities, kersantite dikes cut through quartz syenite and syenite porphyry, as was documented by exploration works and our observations. The true isotopic age of syenitic rocks was probably underestimated, and the age of F–Be ore mineralization testifies to the same.

The genetic or paragenetic links between the quartz syenite and syenite porphyry stocks and ore deposits are of no doubt and are supported by the similar Rb–Sr age of both, their localization in the same tectonic setting, and the close spatial relations. Furthermore, the intrusive rocks are enriched in F and Be against the global background and contain the same accessory minerals as occur in orebodies.

CONCLUSIONS

(1) The fluorine–beryllium deposits of the Vitim Highland make up a large ore field and are represented by the feldspar–fluorite–phenakite–bertrandite and thorite–fluorite–phenakite mineral types.

(2) The localization of the deposits is controlled by deep faults that border on both sides the Paleozoic geosynclinal trough and a narrow tectonic inlier of Precambrian rocks within this trough. The local splay zones and the folds in the country metasedimentary rocks cut through by stocks and dikes also have important ore-localizing implications.

(3) The stocks are composed of quartz syenite and syenite porphyry of Early Mesozoic age. At both studied deposits, the intrusive rocks have similar chemical composition, are characterized by elevated alkalinity, and are enriched in F and Be against the global background value.

(4) The F–Be ore mineralization genetically or paragenetically related to the stocks of quartz syenite and syenite porphyry has a Rb–Sr age of 243–257 ± 3 Ma at the Aunik deposit and 260 ± 2 Ma at the Amandak deposit. The deposits were formed in a disturbed tectonic regime during several stages at temperatures of 360–90°C (Aunik) and 290–130°C (Amandak).

ACKNOWLEDGMENTS

I thank V.F. Posokhov for isotopic analysis of rocks and ores.

REFERENCES

1. O. A. Bogatikov, V. I. Gon'shakova, S. V. Efremova, et al., *Classification and Nomenclature of Igneous Rocks* (Nedra, Moscow, 1981) [in Russian].
2. K. B. Bulnaev, "Origin of the Fluorite–Bertrandite–Phenakite Deposits," Geol. Rudn. Mestorozhd. **38** (2), 147–156 (1996) [Geol. Ore Deposits **38** (2), 128–136 (1996)].
3. A. I. Ginzburg, N. P. Zabolotnaya, and I. I. Kupriyanova, *Genetic Types of Hydrothermal Beryllium Deposits* (Nedra, Moscow, 1975) [in Russian].
4. A. I. Ginzburg, N. P. Zabolotnaya, and I. I. Kupriyanova, *Origin of Hydrothermal Beryllium Deposits* (Nedra, Moscow, 1977) [in Russian].
5. D. A. Lykhin, V. I. Kovalenko, V. V. Yarmolyuk, and G. S. Ripp, "Age of Ore-Bearing Magmatism at the Aunik Deposit, Western Transbaikal Beryllium Metallogenetic Province," Dokl. Akad. Nauk **392** (2), 230–234 (2003) [Dokl. Earth Sci. **392** (7), 990–994 (2003)].
6. A. S. Nazarova, "Feldspar–Fluorite–Phenakite–Bertrandite Deposits," in *Geology of Rare- Element Deposits* (Nedra, Moscow, 1965), No. 27, pp. 73–97 [in Russian].
7. M. I. Novikova, E. P. Shpanov, and I. I. Kupriyanova, "Petrography of the Ermakovskoe Beryllium Deposit," Petrologiya **2** (1), 114–127 (1994).
8. P. V. Osokin and N. Z. Voyush, *Geologic Map, Scale 1 : 200 000. Map Sheet N-49-XVIII. Explanatory Notes* (Nedra, Leningrad, 1965) [in Russian].
9. *Petrographic Code. Igneous and Metamorphic Rocks* (VSEGEI, St. Petersburg, 1995) [in Russian].
10. V. Zh. Tsybzhitov, "New Data on the Fluorite–Bertrandite–Phenakite Mineral Deposits," in *Evolution of Endogenic Processes and Mineralization in the Transbaikalia* (Ulan-Ude, 1981), pp. 110–115 [in Russian].
11. V. V. Yarmolyuk, B. A. Litvinovsky, V. I. Kovalenko, et al., "Formation Stages and Sources of the Peralkaline Granitoid Magmatism of the Northern Mongolia–Transbaikalia Rift Belt during the Permian and Triassic," Petrologiya **9** (4), 351–380 (2001) [Petrology **9** (4), 302–328 (2001)].
12. A. N. Zanvilevich, B. A. Litvinovsky, and G. V. Andreev, *Mongolia–Transbaikalia Peralkaline Granitoid Province* (Nauka, Moscow, 1985) [in Russian].